Journal of Electronic Materials, Vol. 24, No. 11, 1995

Characterization of Very High Purity InAs Grown Using Trimethylindium and Tertiarybutylarsine

S.P. WATKINS, C.A. TRAN, G. SOERENSEN, H.D. CHEUNG, R.A. ARES, Y. LACROIX, and M.L.W. THEWALT

Department of Physics, Simon Fraser University, Burnaby BC V5A 1 S6

The growth of high purity InAs by metalorganic chemical vapor deposition is reported using tertiarybutylarsine and trimethylindium. Specular surfaces were obtained for bulk 5–10 μm thick InAs growth on GaAs substrates over a wide range of growth conditions by using a two-step growth method involving a low temperature nucleation layer of InAs. Structural characterization was performed using atomic force microscopy and x-ray diffractometry. The transport data are complicated by a competition between bulk conduction and conduction due to a surface accumulation layer with roughly $2–4 \times 10^{12}$ cm^{-2} carriers. This is clearly demonstrated by the temperature dependent Hall data. Average Hall mobilities as high as 1.2×10^5 cm^2/Vs at 50K are observed in a 10 μm sample grown at 540°C. Field-dependent Hall measurements indicate that the fitted bulk mobility is much higher for this sample, approximately 1.8×10^5 cm^2/Vs. Samples grown on InAs substrates were measured using high resolution Fourier transform photoluminescence spectroscopy and reveal new excitonic and impurity band emissions in InAs including acceptor bound exciton "two hole transitions." Two distinct shallow acceptor species of unknown chemical identity have been observed.

Key words: InAs, metalorganic chemical vapor deposition (MOCVD), mobility

INTRODUCTION

Many quantum confined devices such as lasers and high electron mobility transistors make use of the narrow bandgap and high electron mobility of InAs. In addition, there is also continued interest in InAs for magnetic field sensors. It is surprising, therefore, that so little is known of the bulk transport and optical properties of this material. For example, parameters which have been known in GaAs and InP for decades, such as the acceptor and exciton binding energies, have until now been completely unknown in InAs. Because of the very small effective mass of electrons and holes in InAs, the purity of the material must be very high in order to observe excitonic processes. The development of high purity alternate source precursors now provides the possibility to grow very high purity InAs by metalorganic chemical vapor deposition (MOCVD). In addition, the recent advent of Fourier transform PL methods greatly enhances the sensitivity and resolution of PL spectroscopy in the 2–3 μm region.

The electrical properties of bulk InAs grown on GaAs were investigated many years ago using the technique of chloride vapor phase epitaxy (VPE).[1] Wieder reported electron mobilities as high as 1.5×10^5 cm^2/Vs in a 17 μm thick sample. In addition, in that work it was demonstrated that the observed transport data were complicated by the existence of significant conduction in a surface accumulation layer due to the lineup of the surface Fermi level of InAs. From the point of view of determining optical properties, this material, while excellent electrically, is of little use because of residual strain due to the large

(Received March 13, 1995; revised May 8, 1995)

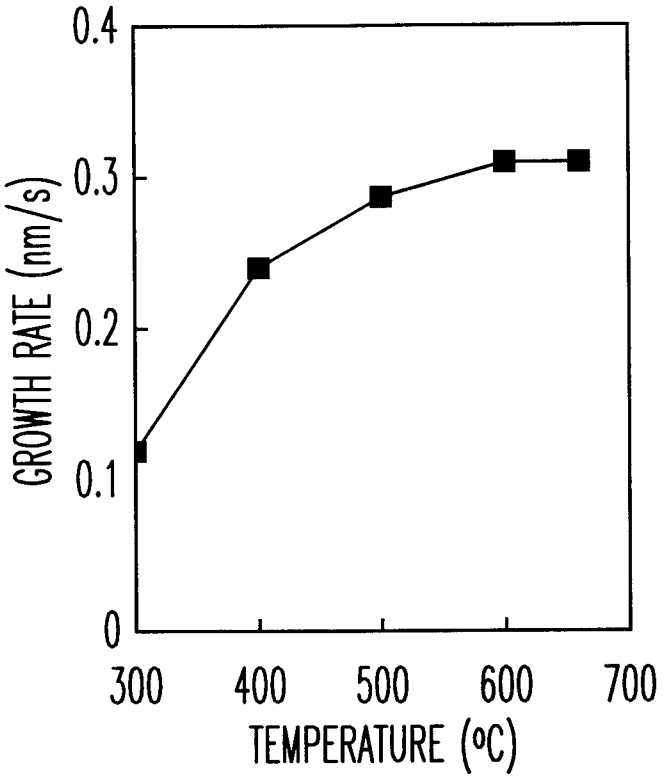

Fig. 1. Summary of InAs growth rate as a function of temperature on InAs substrates.

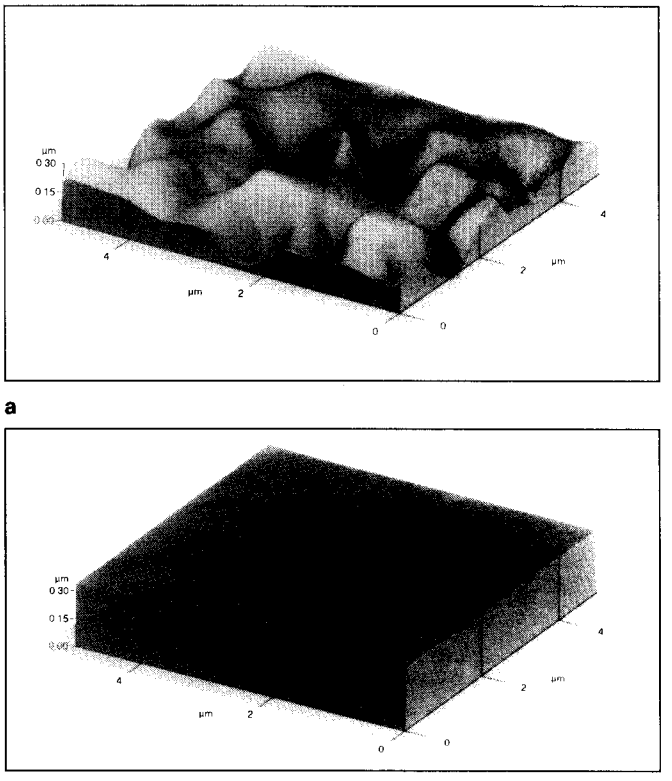

Fig. 2. (a) and (b) compare AFM images of epilayers grown at 540°C without and with the two-step growth method, respectively. The rms roughnesses are, respectively, 80 and 2.1 nm.

7% lattice mismatch with GaAs. There have been very few reported studies on the growth of bulk InAs by MOCVD. Baliga et al.[2] mapped out some of the basic growth and transport properties of the material very early on, but undoubtedly because of source compound limitations, the transport results were greatly inferior to those already obtained by chloride VPE at the time.[1]

More recently, Haywood et al. presented the results of growth of InAs on GaAs using tertiarybutylarsine (TBA) and trimethylindium (TMI) on GaAs substrates,[3] however the surface morphology of the films was adequate over only a very narrow range of growth conditions and the electrical properties were not as good as the best molecular beam epitaxy (MBE) or VPE results. A few other studies[4–6] have reported growth of InAs using trimethylindium and arsine on GaAs substrates, however, the electrical data to date have been greatly inferior to the VPE work, or the best MBE growth results.[7] Some photoluminescence results for InAs epitaxy on InAs and GaAs have been reported,[8–10] but none have reported clearly identifiable sharp line excitonic and impurity emissions of the type well known in GaAs and InP.

In this work, we report the growth of high mobility bulk InAs on GaAs and InAs substrates by (MOCVD) using TBA and TMI. A two-step growth method was found which gave specular epilayers simultaneously on GaAs and InAs substrates over a wide range of growth conditions. The structural properties of the InAs epilayers was studied using atomic force microscopy (AFM) and double crystal x-ray diffraction. The transport properties represent a significant improvement over previously reported values in MOCVD-grown InAs and are comparable to the best ever reported by any growth technique. The resulting material quality has enabled the first observation of many basic optical properties in this material including donor-acceptor pair bands, and extremely sharp bound exciton emission lines. In addition, we present the results of secondary ion mass spectroscopy (SIMS) as a function of growth conditions.

EXPERIMENTAL

InAs epilayers were grown in a vertical downward flow reactor with the substrate mounted horizontally on a Mo susceptor. The inside diameter of the chamber is 6.2 cm. The Mo susceptor is heated radiatively from below by a resistance heater. Temperature control is achieved with a Vanzetti Systems optical pyrometer. The TMI and TBA were maintained at bath temperatures of 18 and 10°C, respectively. Total reactor hydrogen flows of 2.3 standard liters per minute were employed at a pressure of 50 Torr. Hall samples were grown on vertical gradient freeze (100) undoped GaAs semi-insulating substrates miscut 2° toward (110). The best PL samples were grown on undoped liquid encapsulated Czochralski, nominally exact (100) InAs substrates, with residual n-type carrier concentrations of around 2×10^{16} cm^{-3} and a dislocation density of $<10^4$ cm^{-2}. Substrates were cleaned and etched using the method described by Ma

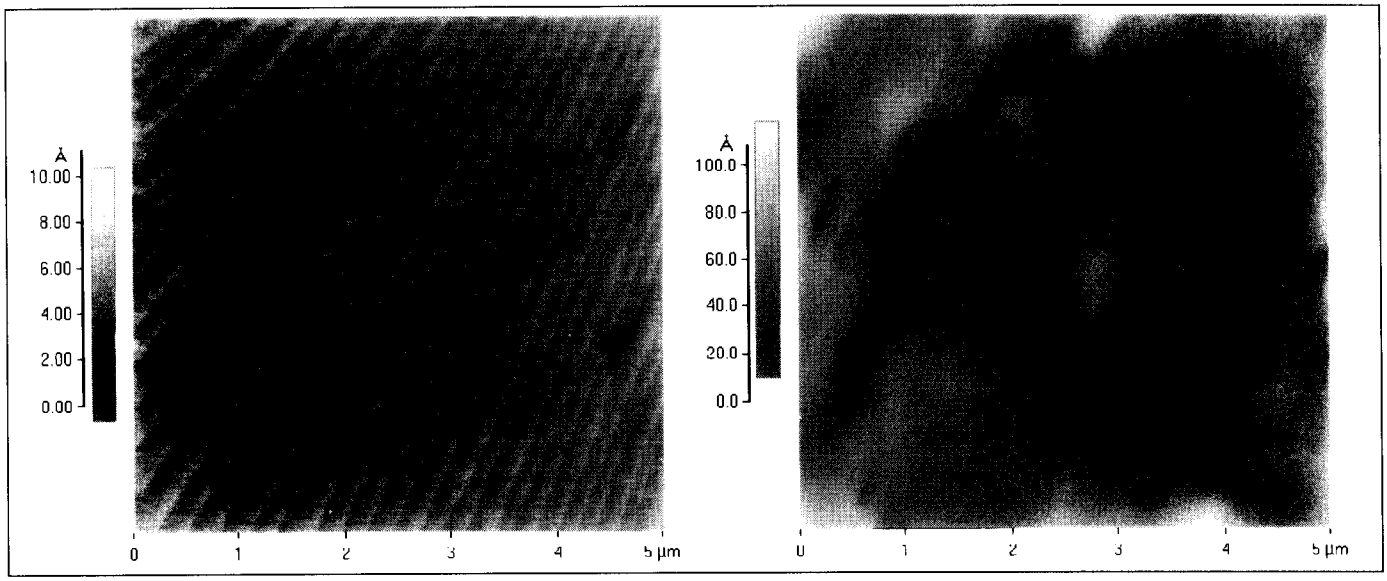

Fig. 3. (c) and (d) compare AFM images of layers 301-1 and 301-2 grown simultaneously during the same run at 540°C but on InAs and GaAs substrates, respectively.

Table I. Transport and Structural Data as a Function of Epilayer Thickness for Growth at 540°C

Run	T_g (C)	P_{TBA} (Torr)	t_e (µm)	μ_H(50K) (10^3cm²/Vs)	n_S(50K) (10^{12} cm^{-2})	n_s(293K) (10^{12} cm^{-2})	Dislocation Density (10^8 cm^{-2})	rms Roughness (nm)	(004) Width (arc sec)
182	400	0.12	0.1	3.1	3.4	3.9	n/a	n/a	n/a
299	540	0.12	0.5	4.5	3.9	4.1	6	4.3	632
300	540	0.12	2.5	23	1.2	3.4	2.6	2.1	248
301	540	0.12	5.0	44	1.0	4.3	1.0	1.3	170
302	540	0.12	10	120	0.59	3.5	0.5	0.74	107

et al.[12] Hall measurements were generally performed at very low fields (100G) in order to minimize the contribution due to surface conduction as described in detail below. Hall measurements were performed no less than 24 h after contact formation because of a previously noted change in the transport values with time immediately following contact formation.[12] The cause of this change is surface related and is currently under investigation. X-ray measurements were performed with a BEDE 150 diffractometer modified to include a four bounce Ge monochromator. Photoluminescence data were obtained using a Bomem DA8 Fourier transform spectrometer fitted with a liquid nitrogen cooled InSb detector. Surface morphologies were measured using a Park Scientific Autoprobe CP AFM operating in air in contact mode. Secondary ion mass spectroscopy (SIMS) measurements were performed by Charles Evans Associates using a Cameca IMS-4f instrument using cesium bombardment.

RESULTS

Structural Characterization

The growth rate of InAs on InAs was found to be diffusion limited for temperatures above 450°C in agreement with Fang et al.[9] Growth rate data for thin InAs on InAs calibration structures are shown in Fig. 1. Growth rates were measured by x-ray diffractometry. Thin, four monolayer InP marker layers were inserted prior to InAs deposition in order to observe interference fringes around the principal (004) Bragg peak. Below 400°C, the growth rate strongly decreased with temperature, indicating incomplete decomposition of the TMI.

Preliminary InAs layers grown directly on GaAs substrates were found to give very rough surfaces as indicated by the AFM image shown in Fig. 2a. Attempts to improve these surfaces by lowering growth rates, and other growth conditions were unsuccessful. Following techniques used in other works on growth of strongly mismatched materials, we found that the growth of a thin 100 nm nucleation layer at 400°C at a low growth rate of 0.3nm/s was successful in maintaining specular surface morphologies in layers up to at least 10 µm in thickness. Prior to deposition of the low temperature layer, the substrate was heated to 540°C under TBA for 5 min in order to clean the surface. Following deposition of the low temperature layer, the wafer was heated to the final growth temperature under TBA. Typical growth rates for temperatures above 500°C were 0.6 or 1.2 nm/s with a TMI flow of 60 or 120 sccm. Figure 2b shows the dramatic improvement in flatness obtained by implementing this two-step procedure. Both (a) and (b) are

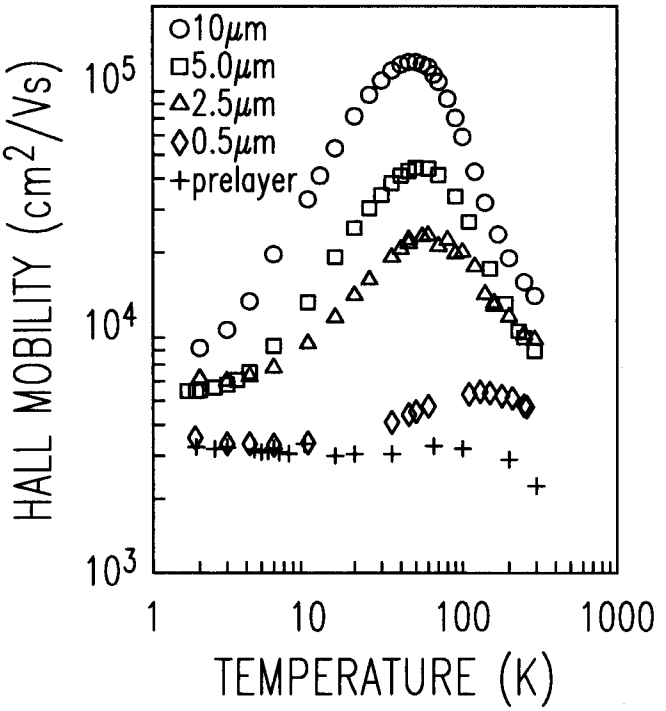

Fig. 4. Hall mobility vs measurement temperature for various epilayer thicknesses grown under identical growth conditions. The growth temperature was 540°C.

displayed with the same z axis dynamic range. Samples grown by this method were mirror-like to the naked eye, and generally showed very few, if any defects by Nomarski microscopy (1000X).

Although the improvement represented by Fig. 2 is dramatic, the surfaces of the InAs samples grown on GaAs are not as flat as those grown on InAs substrates on an atomic scale. Figures 3a and 3b compare AFM images of InAs layers 301-1 and 301-2 grown, respectively, on InAs and GaAs substrates. Both samples were grown during the same growth run (301) and were subjected to the same two-step growth procedure. The samples grown on nominally exact (001) InAs show regular monolayer terraces typical of step flow growth and from which we can infer an unintentional substrate misorientation of approximately 0.18°. The measured rms surface roughness for these layers was 0.09 nm. In contrast, the samples grown on GaAs substrates miscut 2° from (001) show no clear evidence of terraces within the x-y resolution of this scan, but show a significant increase in surface roughness to around 1.3 nm. Several depressions are evident in the InAs on GaAs samples, typified by Fig. 3b, which are attributed to threading dislocations. The observed dislocation density of roughly $1 \times 10^8 cm^{-2}$ is consistent with other reported studies on relaxed growth on highly mismatched substrates e.g. GaSb on GaAs, which has a similar lattice mismatch.[13] Table I shows a summary of transport and structural data on four samples grown under the same growth conditions but with nominal thicknesses of 0.5, 2.5, 5.0, and 10 μm, respectively. The dislocation density decreases somewhat with epilayer thickness but still remains high after 10 μm. Dislocation data were based on four separate 5 μm by 5 μm scans for each sample. Coincident with the decrease in the dislocation density, the rms roughness of this series of samples over a 5 μm by 5 μm region decreases significantly with increasing epilayer thickness reaching a value of 0.74 nm for the 10 μm sample.

Table II. Summary of Growth Conditions, Electrical Properties, and Surface Morphologies of Selected 5 μm InAs Epilayers

Run	T_g (°C)	P_{As} (Torr)	n_s(77K) ($10^{12}cm^{-2}$)	μ_{77} (10^4cm^2/Vs)	Morphology*
204	610	0.12	n/a	n/a	h
194	570	0.12	0.65	5.1	s
200	570	0.028	0.57	3.7	s
203	570	0.014	n/a	n/a	h
269	540	0.12	2.0	7.0	s
193	530	0.12	1.9	6.2	s
195	530	0.028	0.81	5.6	s
196	530	0.014	n/a	n/a	d
197	490	0.12	1.4	3.3	s
201	490	0.028	1.7	2.3	s
199	450	0.12	1.6	2.9	s
198	450	0.028	n/a	n/a	h

Note: Hall data were not taken for samples with poor morphologies.*Appearance to naked eye: s = specular, h = shiny but hazy, d = completely dull, nonspecular.

Table I also shows a summary of the full width at half maximum of the rocking curve of the principal (004) Bragg peak of several layers of different thicknesses grown under the same conditions. There is a marked decrease in the linewidth with increasing thickness to as little as 107 arc sec for the 10 μm layer. This is probably still an over estimate given that the x-ray penetrate several microns into the material for this diffraction angle.

Table II gives a summary of morphology and transport data as a function of growth conditions for several selected 5 μm InAs epilayers on GaAs substrates. Surface quality was categorized according to visual appearance with the naked eye. Specular surface morphologies were obtained over a wide range of growth conditions. InAs substrates were included in each growth run and the surface quality of growths on InAs were always as good or better than those on GaAs. The surfaces of epilayers grown on the two substrates were usually indistinguishable by the naked eye, except near the extremes of growth temperature or low V:III ratio, where the samples grown on InAs were generally superior. In general, specular surfaces were obtained for the highest group V partial pressures from 450 up to 580°C. As the TBA partial pressure was reduced, the morphology suffered. At a temperature of 570°C, this deterioration did not occur until the very low value of 0.014 Torr.

Transport Results

Table II lists the transport properties of several 5

μm epilayers grown as a part of this study. In general, there was little change in the sheet concentration as a function of growth conditions. This is due to the presence of a surface accumulation layer described in more detail below. Nevertheless, a peak was observed in the Hall mobilities in the region of 540°C and this growth temperature was, therefore, selected for the detailed temperature dependent and field dependent transport measurements which follow.

The transport properties of bulk InAs are complicated by the existence of a surface accumulation layer due to the presence of a high density of surface states with energies above the bulk conduction band. A review of the situation has been given by Stradling.[13] The surface accumulation layer results in a relatively low mobility parallel conduction path which can dominate the electrical properties of high purity samples. This was well documented in several early works on very high purity InAs grown by chloride VPE on GaAs.[1] In this work, we report the growth of comparable material by MOCVD. In addition, we are able to explain the rather unusual temperature dependence quite simply in terms of the standard two-layer model. InAs can be represented as a two carrier system consisting of a thin layer at the surface with a sheet concentration n_s and a low surface mobility μ_s, in parallel with a thick high mobility bulk region (the epilayer) with mobility μ_b and sheet concentration n_s. We assume that the contribution from a third layer at the GaAs/InAs interface is negligible due to the very low mobility expected from this heavily dislocated region. For high purity InAs with a bulk carrier concentration of less than 10^{15} cm^{-3}, the bulk Hall mobility should become very large, larger than the case of comparably doped wider gap materials such as GaAs. In contrast, the mobility of the surface layer should be relatively low due to the high density of charged surface states responsible for the accumulation layer. Measurements on VPE and MBE InAs place this surface mobility at around 1–2 × 10^4 cm^2/Vs,[1,7] and this is expected to be independent of temperature as in the case of a three-dimensional degenerate electron gas.

Figure 4 shows the temperature dependent mobility data taken at a field of 100G for the series of samples from Table I which were grown for different thicknesses at a temperature of 540°C. For reference, the data for the 400°C prelayer alone are also given. This sample displays no temperature dependence of the mobility since it is dominated by the surface accumulation layer. At temperatures between 50–100K, the bulk mobility becomes very large in InAs. As a result, as the layer thickness is increased, a larger and larger fraction of the total electron current can pass through the high mobility bulk region. The reason for the large increase in mobility for Fig. 4 with increasing sample thickness, is not due to increasing purity but rather to a lesser and lesser contribution from the low mobility surface layer as the sample thickness is increased. At high and low extremes of temperature, the bulk mobility is fairly low and comparable to the surface value. These two temperature extremes can be used to estimate the magnitude of the surface mobility which can be seen to be of the order of 1 × 10^4 cm^2/Vs.

Figure 5 shows a summary of the measured sheet concentration at 100G for the same series of samples as a function of temperature. The thinnest layers show no temperature dependence of the carrier concentration as expected. The data in Fig. 5 give the initially surprising result that the sheet concentration actually decreases with increasing epilayer thickness. Again, the explanation arises from the fact that between 50–100K, the bulk mobility becomes so high that a large fraction of the current can flow through the bulk region. Since this region of the sample has a much lower sheet concentration of donor electrons, the experimentally observed sheet concentration actually decreases quite substantially over this range compared with the value observed at high or low temperatures. Of course, this decrease would not continue indefinitely, and the detailed dependence of the sheet concentration on thickness can be modeled using theoretical expressions given below. The low temperature sheet concentrations provide a good estimate of the actual surface contribution to the sheet concentration. It is worth noting that the observed sheet concentration for 500 μm thick InAs substrate material showed virtually no change in sheet concentration as a function of temperature. That material had a bulk concentration of 4 × 10^{16} cm^{-3} at 250K. In addition, the Hall mobility and its temperature variation were much smaller for this thick sample and qualitatively different from our epitaxial samples.

The field used for the previous measurements was

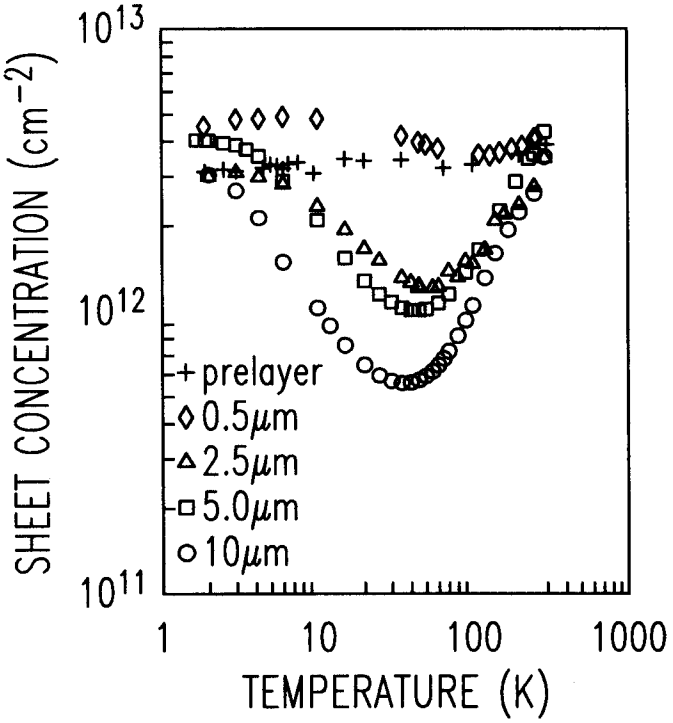

Fig. 5. Sheet concentration vs temperature for the samples shown in Fig. 4.

only 100G. Figure 6 shows the relative changes in the measured Hall mobility μ_{ex} and sheet concentration n_{ex} for the 10 μm sample 302 as a function of field at 50K, where the bulk mobility is near its maximum. Fields above 500G result in a strong drop in the observed Hall mobility and a strong increase in the apparent sheet concentration. These dramatic changes in n_{ex} and μ_{ex} as a function of field are further confirmation of the existence of two separate conduction channels. In contrast, InAs samples deliberately doped with sulfur up to a bulk concentration of 10^{17} cm^{-3} showed a variation in the Hall mobility and sheet concentration of only a few percent over the range 100–6000G, as expected for a single layer system.

The field dependence of the total sheet carrier concentration, for the case of two conductive layers with surface and bulk sheet densities and mobilities n_s, n_b, μ_s, μ_b is given by

$$n_t = \frac{(n_s\mu_s + n_b\mu_b)^2 + \mu_s^2\mu_b^2(n_s + n_b)^2B^2}{n_s\mu_s^2 + n_b\mu_b^2 + \mu_s^2\mu_b^2(n_s + n_b)B^2}. \quad (1)$$

This expression allows for both interplane and intraplane conduction. The measured Hall mobility is related to this expression by

$$\mu_t = \frac{n_s\mu_s + n_b\mu_b}{n_t}. \quad (2)$$

The solid lines in Fig. 6 represent least squared fits obtained using the above expressions for μ_t and n_t. The bulk mobility and bulk sheet concentration were allowed to vary as adjustable parameters, while the surface mobility and sheet density were fixed at 1×10^4 cm^2/Vs and $3.0 \times 10^{12} cm^{-2}$ based on the low temperature limits of Fig. 4 and Fig. 5 for this sample. The best fit was obtained using a bulk mobility of 1.8×10^5 cm^2/Vs with a bulk carrier density of around $2.5 \times 10^{14} cm^{-3}$. The resulting fit is quite good considering the simplification of the model, which does not include contributions from the heavily dislocated GaAs/InAs interface layer. In the limit of low fields, expressions (1) and (2) greatly simplify and can be used to give quite reasonable fits to the observed thickness dependence of the sheet concentration and mobility for the data in Table I.

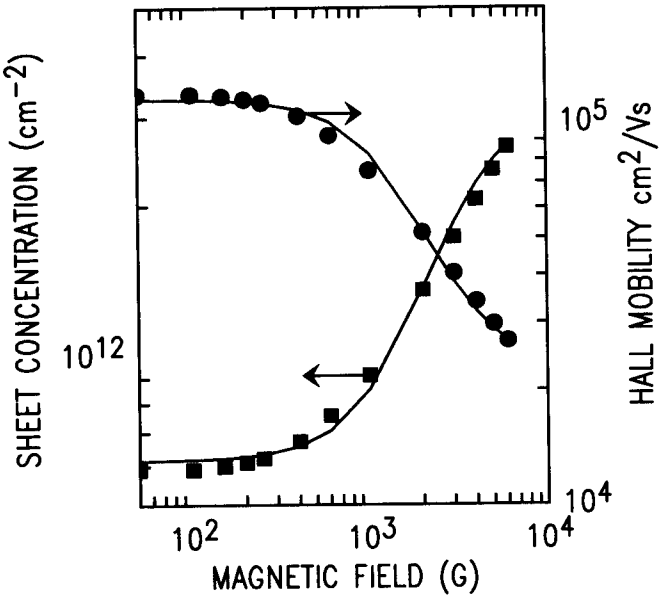

Fig. 6. Experimental mobility and sheet concentration as a function of magnetic field at 50K for the 10 μm sample 302. Solid lines represent a least squared best fit using the expression described in the text. The best fit was obtained with a bulk concentration of $2.5 \times 10^{14} cm^{-3}$ and a bulk mobility of 1.8×10^5 cm^2/Vs.

Secondary Ion Mass Spectrometry

From an inspection of Table II, it is apparent that Hall characterization is of little benefit in making quantitative conclusions regarding impurity incorporation as a function of growth conditions. The presence of the surface accumulation layer strongly masks growth induced changes in the transport properties of high purity InAs with residual bulk carriers below 10^{16} cm^{-3}. The Hall mobility peaks at around 540°C, but no major changes in the total sheet concentration were observed. In order to try to quantify residual impurity incorporation, we performed SIMS profiles of two samples grown at two different TBA partial pressures. These structures consisted of several 100 nm layers grown at temperatures of 600°C down to 400°C in decreasing intervals of 50°C. Carbon and sulfur were chosen for the profiles, as these are known to be common contaminants of InAs and GaAs especially at low temperatures. Table III gives a summary of the observed impurity concentrations. Data obtained for the last layer (400°C) may be affected by surface contamination and should be treated as upper limits on the actual concentration. The two samples were grown at TBA partial pressures of 0.12 and 0.028 Torr, respectively. For the sample grown at the

Table III. Summary of SIMS Measurements for Two Test Structures Grown at Two Different TBA Partial Pressures

		Sample 1: P_{TBA} = 0.12 Torr		Sample 2: P_{TBA} = 0.028 Torr	
Layer	T_G (°C)	C (cm^{-3})	S (cm^{-3})	C (cm^{-3})	S (cm^{-3})
1	400	2×10^{17}	5×10^{16}	5×10^{18}	1×10^{17}
2	450	3×10^{16}	1×10^{16}	1×10^{18}	3×10^{16}
3	500	2×10^{16}	3×10^{15}	1×10^{17}	4×10^{15}
4	550	2×10^{16}	2×10^{15}	4×10^{16}	3×10^{15}
5	600	2×10^{16}	2×10^{15}	2×10^{16}	2×10^{15}

higher partial pressure, sample 1, sulfur and carbon incorporation were at or close to the detection limit down to 450°C. This result is confirmed by the excellent quality of the PL emission from 450°C InAs described below.

For the structure grown at low TBA partial pressure, sample 2, significantly higher levels of carbon and sulfur were observed. It is interesting to observe that carbon incorporation appears to have the same dependence on group V partial pressure as in GaAs even though there is evidence that it forms a donor in MOCVD grown InAs[9] rather than an acceptor. This effect is probably explained in terms of a similar argument to the one employed for GaAs, namely that residual carbon radicals from TMI are removed by reaction with AsH_x species from the TBA. The sulfur concentration decreases rapidly with increasing temperature as expected from thermodynamic arguments. In agreement with Fang et al.,[9] we observe a strong increase in carbon incorporation at low growth temperatures in the case of the structure grown at the lowest TBA partial pressure.

Photoluminescence Results

There are very few previous reports of PL results in InAs. Some measurements were taken on epilayers grown on GaAs substrates, in which case strain effects would be expected to seriously degrade any excitonic or donor acceptor pair spectra.[8,10] Other reports of growth of InAs substrates were performed at relatively low resolution;[9] and in addition, it is likely that the source material purity has not, until recently, been adequate to observe excitonic effects in this material. Several peaks have been reported with linewidths of the order of tens of meV,[8,10] however the physical origin of these were never determined conclusively, nor were any of the very sharp luminescence lines typically observed in GaAs and InP at low temperature observed. The narrow band gap of InAs places stringent purity requirements for the observation of bound donors and bound excitons. Recently Lacroix et al.[15] reported the observation of extremely sharp PL features in InAs grown on InAs substrates which were identified as due to free excitons, acceptor bound excitons, and donor acceptor pair transitions. In this work, we provide some additional data regarding PL at different growth temperatures.

In performing PL measurements on InAs epilayers, we found that the choice of the substrate material is rather important. Early growths were performed on heavily p-type Zn-doped material. The resulting PL showed some very sharp line structure, but was very weak, presumably due to the formation of a p-n junction with the epilayer. Subsequent growths were performed on high quality undoped InAs with residual n-type doping levels of around 1–4 x 10^{16} cm^{-3}.

Figure 7c shows a spectrum obtained for a high purity 5 μm InAs sample grown on undoped InAs at 580°C and a TBA partial pressure of 0.028 Torr. The spectrum is very similar to that of well known PL spectra in GaAs and InP. The identity of the peaks has

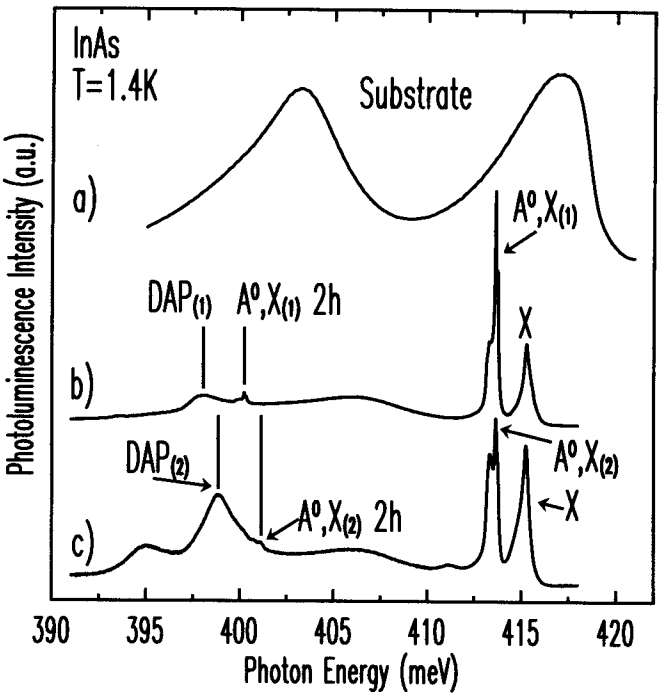

Fig. 7. (b) and (c) show PL spectra of two representative samples at growth temperatures of 450 and 540°C showing excitonic and pair emission spectra at these two widely different growth temperatures. For comparison, the spectrum of a piece of n-type substrate material ($n = 4 \times 10^{16}$ cm^{-3}) is shown in (a).

been briefly reported elsewhere.[15] In summary, the broad band at 397 meV has been identified as a donor acceptor pair band based on the observed blue shift with increasing laser power. The very sharp peak at 413 meV has been identified as due to acceptor bound exciton (A^oX) emission based on the observation of a "two hole" satellite at 400 meV due to the recombination of acceptor bound excitons leaving the acceptor in a $2S_{3/2}$ final state rather than the usual $1S_{3/2}$ final state of the principal A^oX transition. The high energy peak at 415 meV was originally attributed to the free exciton polariton (FE). However, new measurements performed at high magnetic fields indicate that the peak is due to donor bound exciton emission. Further results on this emission line will be presented elsewhere.

Figure 7b shows the PL spectrum of a sample grown at a much lower temperature of 450°C and a TBA partial pressure of 0.12 Torr which also shows extremely sharp and well resolved excitonic features, including a well resolved two-hole feature. The high quality of this spectrum confirms the SIMS data which showed that residual carbon and sulfur levels are very low even at those low growth temperatures. For comparison, the PL spectrum of a piece of substrate material is included in Fig. 7a in order to emphasize the significant improvement in material quality for the epitaxial layers.

The $1S_{3/2}$-$2S_{3/2}$ energy splitting of the low temperature sample is 13.39±0.01 meV which agrees with the value reported in Ref. 15. In the high temperature sample in Fig. 7c, the location of the two-hole transition is slightly shifted with respect to the 450°C

sample. Based on the separation from the principal A°X peak, this peak corresponds to a new shallower acceptor with a $1S_{3/2}$ to $2S_{3/2}$ energy difference of 12.54 ±0.01 meV. For both of the acceptors shown in Fig. 7, the observed energy difference is close to the theoretical effective mass value of 11.31 meV[16] thereby conclusively identifying the sharp line transition labeled A°X as an acceptor bound exciton and not a donor bound exciton, for which the $1S_{3/2}$-$2S_{3/2}$ energy difference should be far smaller. These results demonstrate that chemical central cell shifts between different acceptors in InAs are observable despite the very small bandgap and light electron and hole effective masses. The chemical identity of these two shallow acceptors is unknown at present and will require careful backdoping studies. GaAs epilayers grown with the current sources typically show PL emission due to low levels of residual Zn, therefore this is a likely choice for one of the observed acceptors.

SUMMARY

In summary, we have reported the growth of structurally excellent InAs on GaAs as determined by surface morphology and x-ray diffraction linewidths. We have observed very good transport properties as confirmed by the variation of the Hall data with temperature, reaching mobilities of up to 1.2×10^5 cm^2/Vs at 50K in a 10 μm sample. The observed mobilities are clearly limited by surface effects and not by the impurity content of the layers. A bulk mobility of 1.8×10^5 cm^2/Vs was deduced from magnetic field dependent transport measurements for the 10 μm sample. The unusual temperature dependent Hall data are quite consistent with previous models for two-layer conduction in InAs. The significant improvements in material quality have been used to observe sharp excitonic emission in InAs, allowing determination of acceptor binding energies for this material. Photoluminescence measurements show that very high purity material can be grown at temperatures as low as 450°C. Two distinct acceptor species of unknown chemical origin have been observed through their two hole transitions.

ACKNOWLEDGMENTS

The support of the Natural Sciences and Engineering Research Council of Canada (NSERC) and the British Columbia Ministry of Training and Education is gratefully acknowledged. One ofthe authors (CAT) would like to acknowledge financial support from the Fonds pour la Formation des Chercheurs et l'aide à la Recherche (FCAR), Gouvernement de Québec.

REFERENCES

1. H.H. Weider, *Appl. Phys. Lett.* 25, 206 (1974).
2. B.J. Baliga and S.K. Ghandi, *J. Electrochem. Soc.* 121, 1642 (1974).
3. S.K. Haywood, R.W. Martin, N.J. Mason and P.J. Walker, *J. Electron. Mater.* 19, 783 (1990).
4. S. Kalem, J. Chyi, C.W. Litton, H. Morkoç, S.C. Kan and A. Yariv, *Appl. Phys. Lett.* 53, 562 (1988).
5. D.L. Partin, L. Green, D.T. Morelli, J. Heremans, B.K. Fuller and C.M. Thrush, *J. Electron. Mater.* 20, 1109 (1991).
6. Y. Iwamura, H. Shigeta and N. Watanabe, *Jpn. J. Appl. Phys.* 32, part 2, L368 (1993).
7. P.D. Wang, S.N. Holmes, Tan Le, R.A. Stradling, I.T. Ferguson and A.G. Oliveira, *Semicond. Sci. and Technol.* 7, 767 (1992).
8. R.D. Grober and H.D. Drew, *J. Appl. Phys.* 65, 4079 (1989).
9. Z.M. Fang, K.Y. Ma, R.M. Cohen and G.B. Stringfellow, *Appl. Phys. Lett.* 59, 1446 (1991).
10. P.J.P. Tang, C.C. Phillips and R.A. Stradling, *Semicond. Sci. Technol.* 8, 135 (1993).
11. D. Brar and D. Leonard, *Appl. Phys. Lett.* 60, 463 (1995).
12. K.Y. Ma, Z.M. Fang, R.M. Cohen and G.B. Stringfellow, *J. Appl. Phys.* 68, 4587 (1990).
13. R.A. Stradling, *Growth and Characterization of Semiconductions*, ed. R.A. Stradling and P.C. Klipstein, (Bristol: Adam Hilger, 1991), p. 170.
14. S.P. Watkins, C.A. Tran, R. Ares and G. Soerensen, *Appl. Phys. Lett.* 66, 882 (1995).
15. Y. Lacroix, S.P. Watkins, C.A Tran and M.L.W. Thewalt, *Appl. Phys. Lett.* 66,1101 (1995).
16. A. Baldereschi, *Phys. Rev. B* 9, 1525 (1974).